

Translational Relevance

For therapies using EGFR-TKIs (e.g., gefitinib and erlotinib), it is essential to determine the epidermal growth factor receptor mutation status of lung cancer lesions. Although a biopsy of the primary lesion is indispensable, noninvasive diagnostics are desirable because they allow repeated testing. In particular, it is useful to follow the disease progression by monitoring the T790M status. In contrast to other techniques, beads, emulsion, amplification, and magnetics (BEAMing) can estimate the extent to which the activating mutation alleles have been converted into resistant alleles, regardless of normal DNA contamination. This information should be more suitable for monitoring the disease status. Because BEAMing also detects activating mutations with a moderate success rate, examining the ctDNA may support a diagnosis via a biopsy. It should be noted that BEAMing and next-generation sequencers are based on the same technological principle. With this study, we can predict how next generation sequencers will detect mutations in circulating tumor DNA.

products amplified from a single molecule are fixed to a single magnetic bead using emulsion PCR. The mutation site is labeled with a fluorescent probe or primer extension, and the mutated allele is quantitatively detected by counting the fluorescently labeled beads. Simply by increasing the number of beads that are analyzed, BEAMing can be more sensitive than other PCR-based techniques (13).

In this report, we used BEAMing to detect activating and resistant *EGFR* mutations in ctDNA derived from lung cancer. The results suggest that ctDNA may complement the biopsy of primary lesions as a source of *EGFR* mutation detection. Its major advantage over other techniques is its ability to calculate the fraction of T790M-positive alleles in cancer cells, regardless of normal cell DNA contamination. In particular, this approach would enable the monitoring of disease progression during EGFR-TKI therapy via the T790M mutation.

Materials and Methods

Patient characteristics

Patients with activating *EGFR* mutations in tumor tissues were selected following a biopsy examination between June 2010 and April 2011. We recruited 23 patients with progressive disease (PD) after EGFR-TKI treatment as group 1. PD is defined as the appearance of a new lesion or a 20% increase in tumor size. The duration between the detection of PD and blood sampling for BEAMing was variable. We recruited 21 patients who had never been treated with EGFR-TKIs as group 2. In all of the patients, activating *EGFR* mutations were found in biopsy samples using the PNA-LNA PCR clamp method (14).

Plasma samples and DNA extraction

DNA was purified from plasma obtained from 5 mL of heparin-treated blood using Agencourt Genfind version 2 (Beckman Coulter). The DNA concentration was determined by measuring the copy number of *LINE-1* (15). It should be noted that the calibration was done using intact human genomic DNA, whereas the plasma DNA was in fragments of approximately 200 bp or less. Thus, the deduced measurement may be biased to be too low.

BEAMing

BEAMing was done as described previously (16, 17), except for the use of locked nucleic acids (LNA) as the hybridization probes for single-base substitutions. Primer and probe sequences are shown in Table 1. In the initial PCR step, the target region (~100 bp) was amplified using gene-specific primers with tag sequences. Amplification was done in a 100- μ L reaction mixture containing genomic DNA obtained from 400 μ L of plasma, 600 pmol of primers and 2 units of KOD -Plus- DNA polymerase (Toyobo). The product was purified with a MinElute PCR Purification Kit (Qiagen).

To prepare the magnetic beads for BEAMing, a common oligonucleotide, the sequence of which was identical to the forward primer for emulsion PCR (Table 1), was synthesized using a dual biotin group at the 5' end and a spacer 18 polyethylene glycol between the biotin group and the terminal thymidine (Integrated DNA Technologies). One nanomole of the common oligonucleotide was attached to 100 μ g of MyOne streptavidin-coated magnetic beads (Dynal), as described previously (12). The beads were finally suspended in 100 μ L of TK buffer (20 mmol/L Tris-HCl, pH 8.4, 50 mmol/L KCl). To prepare the emulsifier oil, 7% ABIL WE09 (Degussa), 20% mineral oil (Sigma-Aldrich) and 73% Tegosoft DEC (Degussa) were mixed by vortexing and allowed to settle for 30 minutes.

Emulsion PCR was done as follows. A 150- μ L reaction mixture consisted of 15 μ g of the first aforementioned PCR product, 15 μ L of 10 \times KOD buffer, 75 pmol of the forward primer, 12 μ mol of the reverse primer and 6 μ L of the magnetic beads, which were prepared as described above. Next, 0.6 mL of the emulsifier oil and 5-mm Zirconia beads were added to the 150- μ L reaction mixture. A water-oil emulsion was prepared in a 2-mL Eppendorf tube using a Mixer Mill MM 300 (Qiagen) at 15 Hz for 17 seconds. The reaction mixture was divided into 50- μ L aliquots and amplified using the following thermal cycling protocol: 94°C for 2 minutes; 3 cycles of 98°C for 15 seconds, 64°C for 45 seconds, and 72°C for 75 seconds; 3 cycles of 98°C for 15 seconds, 61°C for 45 seconds, and 72°C for 75 seconds; 3 cycles of 98°C for 15 seconds, 58°C for 45 seconds, and 72°C for 75 seconds; and 50 cycles of 98°C for 15 seconds, 57°C for 45 seconds, and 72°C for 75 seconds.

After thermal cycling, the reaction mixture was centrifuged to separate the oil and water. After removing the supernatant, the emulsion was degraded with 400 μ L of breaking buffer (5 mmol/L Tris-HCl, pH 7.5, 1% Triton X-100, 1% SDS, 100 mmol/L NaCl, 1 mmol/L EDTA) and by

Table 1. Primer list

	Name	Sequence	Modification	Target
Primers for exon amplification from plasma DNA				
exon19	Tag119del	TCCCGCGAAATTAATACGACAAGTTAAAATCCCGTCGCTATC		
	Tag219del	GCTGGAGCTCTGCAGCTAGACCCCCACACAGCAAAG		
exon20	Tag1T790M	TCCCGCGAAATTAATACGACGCATCTGCCTCACCTCCAC		
	Tag2T790M	GCTGGAGCTCTGCAGCTAAGCAGGTAAGTGGAGCCAAT		
exon21	Tag1L858R	TCCCGCGAAATTAATACGACAGCCAGGAACGTACTGGTGA		
	Tag2L858R	GCTGGAGCTCTGCAGCTATGCCTCCTTCTGCATGGTAT		
Primers for emulsion PCR				
	Tag1 (forward)	TCCCGCGAAATTAATACGAC		
	Tag2 (reverse)	GCTGGAGCTCTGCAGCTA		
Hybridization probes for detection of beads with successful amplification				
exon19	19del_BEAM_PE_b	AGCAAAGCAGAAACTCACATC	5' biotin	
exon20	T790M_BEAM_PE_b	CGGACATAGTCCAGGAG	5' biotin	
exon21	L858R_BEAM_PE_b	ATGCCTCCTTCTGCATGGTAT	5' biotin	
Hybridizationprobe for BEAMing				
exon19	19del_35_49_647	GGAGATGTTTTGATAGCG	5' Alexa647	exon 19 E746-A750del
	19del_36_50_647	CGGAGATGTCTTGATAGC	5' Alexa647	exon 19 E746-A750del
	19del_40_57_647	TGGCTTTTCGATTCCTTGA	5' Alexa647	exon 19 L747-S752del.P753S
	19del_AAATTCC_647	TGTTGCTTCTCTTGAATT	5' Alexa647	exon 19 E746-L747del.IP
	19del_36_55_T_647	GCTTTTCGGAACCTTGATAG	5' Alexa647	exon 19 L747-S752del. E746V
	19del_35_53_ACT_647	GGAGAAGTTTTGATAGCG	5' Alexa647	exon 19 K745-E749del.A750K
	19del_39_56_CAG_647	TTTCGGCTGTTTCTTGAT	5' Alexa647	exon 19 L747-T751del.S752Q
	19del_39_48_C_647	GAGATGTTGGTTCCTTGAT	5' Alexa647	exon 19 L747-E749del.A750P
	19del_WT_488	TGTTGCTTCTCTTAATTCC	5' Alexa488	exon 19 wild-type control
	exon20	T790M_Mut_BNA_647	atgagctgcAtgatgag	5' Alexa647
T790M_WT_BNA_488		tgagctgcGtgatgag	5' Alexa488	Wild-type control for T790M
exon21	L858R_Mut_LNA_647	gtttggccCgccccaaat	5' Alexa647	L858R mutation
	L858R_WT_LNA_488	gtttggccAgccccaaat	5' Alexa488	Wild-type control for L858R
	T2582A_Mut_647	caccagcTgtttggcc	5' Alexa647	T2582A mutation
	T2582A_WT_488	caccagcAgtttggcc	5' Alexa488	Wild-type control for T2582A

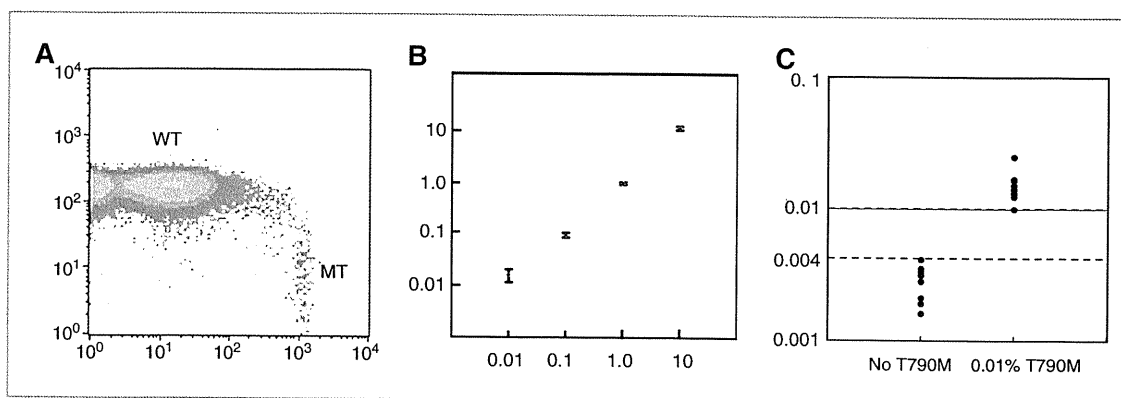


Figure 1. A, flow cytometric profile of BEAMing. The wild-type *EGFR* fragment was mixed with 0.1% of the T790M *EGFR* fragment, and BEAMing was done after PCR amplification. Horizontal axis, the fluorescence intensity of Alexa 647; vertical axis, the fluorescence intensity of Alexa 488. WT, signals from the wild-type *EGFR* fragment; MT, signals from the T789M fragment. B, linear correlation between the inoculated amount of the T790M *EGFR* fragment and the BEAMing measurement. Horizontal axis, the fraction of the T790M fragment inoculated into the wild-type fragment; vertical axis, the fraction of the T790M-positive allele measured using BEAMing. C, repeated measurements of the samples with 0.01% of the T790M fragment and those with no T790M fragment. The vertical axis indicates the fractions of the T790M-positive allele detected using BEAMing.

vortexing. After centrifugation and removal of the supernatant, the beads were washed once. Next, the DNA on the beads was denatured by 2 minutes of incubation at room temperature with 500 μ L of 0.1 mol/L NaOH. After washing twice, the beads were suspended in 30 μ L of distilled water.

The mutation loci were detected using allele-specific hybridization probes that consisted of locked nucleic acids and were fluorescence-labeled at their 5' ends. Alexa 647 and Alexa 488 fluorescent dyes were used for the mutated and wild-type alleles, respectively. A hybridization probe complementary to common sequences in the mutated and wild-type alleles was manufactured via 5' biotinylation. The hybridization reactions were carried out in a 100- μ L reaction mixture consisting of 3 mol/L tetramethylammonium chloride, 50 mmol/L Tris-HCl (pH 7.5), 4 mmol/L EDTA, and 5 pmol each of the aforementioned hybridization probes. The reaction mixture was divided into 50 μ L aliquots, incubated at 70°C for 10 seconds, then at 35°C for 2 minutes after cooling down at a rate of 0.1°C/s, and additionally cooled down to room temperature using the GeneAmp PCR System 9700 Thermal Cycler (Applied Biosystems). After removing the supernatant, the beads were incubated at room temperature for 10 minutes in 20 μ L of binding buffer (5 mmol/L Tris-HCl, pH 7.5, 1 mol/L NaCl, 1 mmol/L EDTA) containing 2 μ g of streptavidin-conjugated phycoerythrin (PE; Invitrogen). After washing, the beads were suspended in 100 μ L of TK buffer. Flow cytometric analysis was conducted with FACSCalibur (BD Bioscience) according to the manufacturer's protocol.

Results

Quantitation of the accuracy and sensitivity of BEAMing

We examined the measurement's accuracy and sensitivity using T790M as an example. We prepared normal *EGFR*

gene fragments containing the mutated fragment at 10%, 1%, 0.1%, and 0.01%. These preparations were subjected to emulsion PCR. A typical example of a flow cytometric profile separating 1% T790M from the wild-type allele is shown in Fig. 1A. In BEAMing, the fractions of the mutated fragment are estimated by the ratio of the numbers of beads labeled with Alexa 647 (mutant) and those labeled with Alexa 488 (wild-type). There is a good linear correlation between the ratio deduced from the numbers of beads and the fraction of mutated fragments in the initial preparations (Fig. 1B). To determine the detection limit of BEAMing, samples without the T790M mutation and samples with 0.01% T790M mutations were analyzed repeatedly. The measurements of these 2 groups did not overlap (Fig. 1C). To confirm this result in a real experimental setting, we measured exon 19 deletion, L858R, and T790M mutations in the plasma DNA purified from 20 normal individuals. The mutation rates ranged from 0 to 0.0094 (average, 0.0021; 95% CI, 0.0012–0.0030), from 0.0009 to 0.0074 (average, 0.0025; 95% CI, 0.0019–0.0031) and from 0.0011 to 0.0097 (average, 0.0042; 95% CI 0.0030–0.0054), respectively. Thus, we set the detection limit of BEAMing as 1 in 10,000.

Activating and resistant *EGFR* mutations in plasma DNA

Plasma obtained from 44 patients was analyzed by BEAMing for the T790M mutation, and activating mutations were determined via a tumor biopsy. The results are shown in Table 2. In group 1, which consisted of patients who developed PD after *EGFR*-TKI treatment, the detection of activating and T790M mutations can be evaluated. In group 2, which consisted of patients who were never treated with *EGFR*-TKI, only those with activating mutations were evaluated. Most of the cases were in stage IV when their plasma DNA was obtained. In 32 of 44 patients, activating

Table 2. Allele frequency of activating and resistant *EGFR* mutations

Patient	Age, y	Sex	Histology	Stage	T790M, %	Activating mutation, %	T790M/activating mutation, %	Activating mutation type
A. Group 1 (patients with PD after EGFR-TKI treatment)								
1	56	M	adeno	4	0.029	0.058	50.8	L861Q
2	58	F	adeno	4	0.26	0.28	94.0	L858R
3	70	F	adeno	4	2.61	7.39	35.3	L858R
4	78	M	adeno	3A	0.08	0.13	65.0	L858R
5	65	M	Adeno + Sq	4	0.63	1.10	57.6	L858R
6	20	M	Adeno	4	0.14	1.03	13.3	exon 19 E746-A750del
7	41	F	adeno	4	4.28	10.3	41.6	exon 19 E746-A750del
8	59	F	adeno	4	9.54	42.7	22.3	exon 19 E746-A750del
9	53	M	adeno	4	0.16	0.19	83.6	exon 19 E746-A750del
10	49	F	adeno	4	ND	0.12	0.0	L861Q
11	75	F	adeno	4	ND	2.03	0.0	L858R
12	34	M	adeno	4	ND	0.33	0.0	L858R
13	64	M	adeno	4	ND	12.2	0.0	L858R
14	73	F	adeno	4	ND	0.046	0.0	L858R
15	66	F	adeno	4	ND	0.28	0.0	exon 19 L747-S752del.P753S
16	70	M	adeno	4	ND	11.5	0.0	exon 19 L747-S752del.P753S
17	44	F	adeno	4	ND	0.09	0.0	exon 19 L747-E749del.A750P
18	52	M	adeno	4	ND	0.74	0.0	exon 19 L747-E749del.A750P
19	74	F	adeno	4	ND	0.33	0.0	exon 19 E746-A750del
20	63	F	adeno	4	ND	ND	NA	L858R
21	65	F	adeno	4	0.10	ND	NA	exon 19 E746-A750del
22	51	F	adeno	4	ND	ND	NA	exon 19 E746-A750del
23	62	F	adeno	4	ND	ND	NA	exon 19 E746-A750del
B. Group 2 (patients not treated with EGFR-TKI)								
24	68	M	adeno	4	ND	0.17	0.0	L858R
25	45	F	adeno	4	ND	0.23	0.0	L858R
26	85	F	adeno	2B	ND	0.25	0.0	L858R
27	67	F	adeno	4	ND	0.079	0.0	L858R
28	58	F	adeno	4	ND	0.013	0.0	L858R
29	39	F	adeno	3B	ND	36.4	0.0	L858R
30	36	F	adeno	4	ND	0.11	0.0	exon 19 L747-S752del.E746V
31	56	M	adeno	4	ND	6.47	0.0	exon 19 L747-T751del.S752Q
32	55	F	adeno	3A	ND	6.24	0.0	exon 19 L747-E749del.A750P
33	65	F	adeno	3B	ND	11.8	0.0	exon 19 E746-A750del
34	76	F	adeno	4	ND	1.06	0.0	exon 19 E746-A750del
35	63	F	Sq	4	ND	0.73	0.0	exon 19 E746-A750del
36	63	M	adeno	4	ND	0.030	0.0	exon 19 E746-L747del.IP
37	72	F	adeno	4	ND	ND	NA	L858R
38	70	F	adeno	4	ND	ND	NA	L858R
39	63	M	adeno	4	ND	ND	NA	L858R
40	80	F	adeno	4	ND	ND	NA	L858R
41	70	F	adeno	4	ND	ND	NA	L858R
42	72	M	adeno	4	0.03	ND	NA	exon 19 L747-S752del.P753S
43	47	M	adeno	4	ND	ND	NA	exon 19 E746-A750del
44	54	F	adeno	4	ND	ND	NA	exon 19 E745-E749del.A750K

Abbreviations: NA, not applicable; ND, not detected.

mutations were detected in the plasma DNA (72.7%; 95% CI, 58.0–83.6%). The detection rate was higher in group 1 (group 1, 82.6%; group 2, 61.9%), but this difference was not statistically significant (the Fischer exact test, $P = 0.18$).

The detection rates of L858R/L861Q and exon 19 deletion were identical (72.7%). The T790M mutation was detected in 10 of 23 patients in group 1 (43.5%; 95% CI, 25.6%–53.4%). Because T790M accounted for about half of the

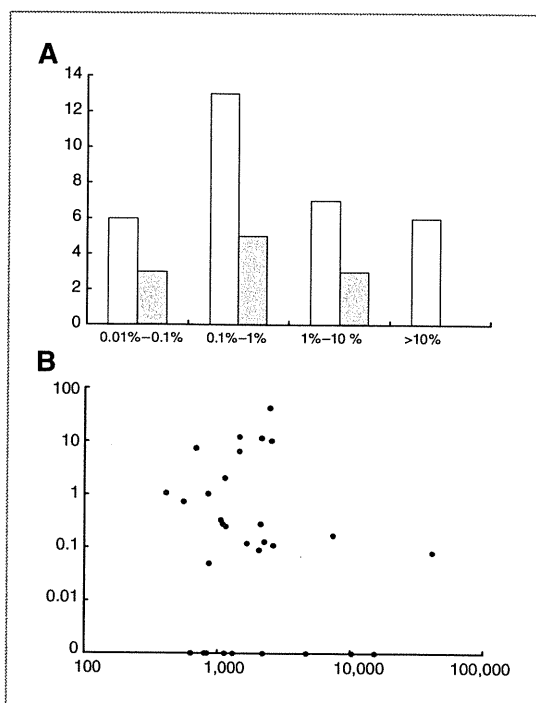


Figure 2. A, distribution of the fraction of *EGFR* molecules with activating (white columns) or resistant (gray columns) mutations in the plasma DNA. Horizontal axis, the percentage of activating *EGFR* mutations; vertical axis, the number of patients. B, relationship between the amount of recovered plasma DNA and the fraction of activating *EGFR* mutations. Horizontal axis, the amount of recovered plasma DNA (pg) corresponding to 400 μ L of plasma; vertical axis, the percentage of activating *EGFR* mutations.

TKI-resistant cases, BEAMing was likely to detect T790M in most of the eligible cases. There were 2 cases of T790M mutations without an activating mutation (i.e., patients 21 and 42).

The fraction of ctDNA in plasma DNA can be estimated from the fraction of *EGFR* mutations [Table 2, activating mutations (%)]. On the basis of the histogram in Fig. 2A, the fraction of activating mutations varied widely across patients, and the peak of the distribution was in the 0.1% to 1% range. The fraction of the T790M mutation was distributed similarly but tended to shift toward lower percentages. We also investigated the relationship between the amount of recovered plasma DNA and the ctDNA deduced from the activating mutations, but we found no relationship between them (Fig. 2B). It should be noted that *EGFR* mutations were not detected in some samples with a high plasma DNA recovery.

We can deduce the number of tumor *EGFR* alleles that have been converted into resistant forms (i.e., T790M) by calculating the ratio of T790M to the number of activating mutation fractions. The ratios were within a range of 13.3% to 94.0% (Table 2), in contrast to a much wider range of tumor alleles in the plasma DNA.

Discussion

There have been a number of studies on the analysis of ctDNA to detect *EGFR* mutations in the serum or plasma DNA of NSCLC patients. These studies have mainly used techniques based on selective amplification (18, 19) or digestion (19) of specific alleles and/or high-throughput separation techniques [i.e., MALDI-TOF (20) or denaturing high performance liquid chromatography (DHPLC) (19, 21)]. The sensitivity is restricted by the specificity of the primers and enzymes in the former and by the signal-to-noise ratio in the latter. Because the sensitivity of BEAMing is only restricted by the mutations introduced during PCR (which is common to all techniques), it is theoretically more sensitive than other methods.

In addition to its high sensitivity, BEAMing allows the digital quantification of mutant alleles. The DNA in blood is derived from both tumor cells and normal cells, but we still do not know how the DNA in blood is generated. The major advantage of BEAMing is its ability to calculate the fraction of T790M-positive alleles from alleles with activating mutations. This feature enables the monitoring of the fractions of the T790M mutation in cancer cells, regardless of normal cell DNA contamination. This information should be more suitable for monitoring disease statuses. Some patients were reported to have cancer cells with T790M as a minor subpopulation before *EGFR*-TKI treatment (22, 23). With these cases, a qualitative assay to monitor T790M is inappropriate, and it is desirable to monitor amount of the T790M allele quantitatively. The fraction of the T790M allele would increase during the *EGFR*-TKI therapy and eventually reach a threshold to acquire resistance. Such threshold can be determined only with a quantitative assay. Partly due to difficulty of the biopsy of recurrent cases, clinical features of T790M-based resistance have not been fully understood, but are currently intensively studied. Such studies would find applications of the quantitative assay. For example, detecting the T790M mutation in blood samples would be useful for patient selection for treatment with new *EGFR*-TKIs for lung cancers that are resistant to gefitinib and erlotinib (24). One of such agents, PF00299804, is effective to a T790M-positive cell line. However, amplification of the T790M allele led to resistant to PF00299804 (25). If PF00299804 acts in patients in the same manner, quantitative monitoring of T790M allele would be useful for detection of resistance. In such patients, a biopsy of the tumor tissue is difficult and noninvasive diagnostics are highly beneficial.

The aim of this study is the initial demonstration of the technique, and has limitations as a clinical study. The patients were not enrolled in this study prospectively, and the timing of blood draws was not consistent such that the results are not directly applicable to distinct clinical situations. In addition, patients did not have serial tumor biopsies to document development of T790M in their cancer after exposure to *EGFR*-TKI. A well-designed prospective study enrolling more than 200 Japanese patients, a population with high incidence of activating mutation, now

being planned to validate present observations. It should be noted that specificity, that is, absence of pseudopositive, is most important for new noninvasive diagnostics. The validation study should also be focused on this point as well.

As suggested by a recent review (26), the most problematic aspect of ctDNA analysis is the difficulty in purifying DNA from the blood. As described above, the amount of plasma DNA varies by 2 orders of magnitude. The cause of this variation (i.e., whether it is due to true variation or the low reproducibility of the purification procedure) is unknown. However, it should be noted that unsuccessful mutation detection was not necessarily frequent in the cases with low DNA recovery and that unsuccessful mutation detection was still found among those with abundant DNA recovery. Some cases of low DNA recovery contained the minimum number of *EGFR* copies for detection. In such cases, whole-genome amplification is beneficial for sound PCR and may enhance the detection rate, as seen in a previous study (19).

This study focused on advanced lung cancer (mainly stage IV lung cancer). If ctDNA analysis is effective for early lung cancer, then it may be applicable to early cancer detection. Because ctDNA is also easily detected in the early stages of colorectal cancer (27), it is worthwhile to test ctDNA analysis for early lung cancer.

BEAMing uses the template preparation step of massively parallel sequencers (so-called next-generation sequencers; ref. 28). Therefore, we can predict the outcome when massively parallel sequencers are applied to this problem. The recent development of a new sequencer (29) has addressed the shortcomings of currently available sequencers (i.e., a long runtime for a single assay and high operating costs), and would be suitable for diagnostic purposes.

The cost of sequencing is still rapidly decreasing, and will be eventually negligible in the total cost of the assay. In contrast to BEAMing, which analyzes only a single base and requires information about mutations in primary tumors, the massively parallel sequencers obtain information from more than a hundred bases and could replace BEAMing. A recent study pointed out the need for repeated sequencing to overcome the high error rates of the sequencers that are currently used to detect rare mutations (30). However, in the case of *EGFR* mutations, because the mutation sites are already known, rare mutations may be detected with a statistical method without the repeated sequencing. Our study forecasts the outcome of ctDNA analysis using massively parallel sequencers, suggesting that ctDNA analysis could determine the *EGFR* mutation status of more than 70% of advanced lung cancer cases. In addition, there might be cases in which *EGFR* mutations could be detected only with ctDNA analysis, not with a conventional biopsy. Given the noninvasive nature of the ctDNA analysis, it is a worthwhile field for future investigation.

Disclosure of Potential Conflicts of Interest

No potential conflicts of interest were disclosed.

Grant Support

This work was partly supported by KAKENHI 20890299 and 23790636.

The costs of publication of this article were defrayed in part by the payment of page charges. This article must therefore be hereby marked *advertisement* in accordance with 18 U.S.C. Section 1734 solely to indicate this fact.

Received July 4, 2011; revised September 20, 2011; accepted September 23, 2011; published OnlineFirst October 5, 2011.

References

- Lynch TJ, Bell DW, Sordella R, Gurubhagavatula S, Okimoto RA, Brannigan BW, et al. Activating mutations in the epidermal growth factor receptor underlying responsiveness of non-small-cell lung cancer to gefitinib. *N Engl J Med* 2004;350:2129–39.
- Paez JG, Janne PA, Lee JC, Tracy S, Greulich H, Gabriel S, et al. *EGFR* mutations in lung cancer: correlation with clinical response to gefitinib therapy. *Science* 2004;304:1497–500.
- Rosell R, Moran T, Queralt C, Porta R, Cardenal F, Camps C, et al. Screening for epidermal growth factor receptor mutations in lung cancer. *N Engl J Med* 2009;361:958–67.
- Kobayashi S, Boggon TJ, Dayaram T, Janne PA, Kocher O, Meyerson M, et al. *EGFR* mutation and resistance of non-small-cell lung cancer to gefitinib. *N Engl J Med* 2005;352:786–92.
- Pao W, Miller VA, Politi KA, Riely GJ, Somwar R, Zakowski MF, et al. Acquired resistance of lung adenocarcinomas to gefitinib or erlotinib is associated with a second mutation in the *EGFR* kinase domain. *PLoS Med* 2005;2:e73.
- Oxnard GR, Arcila ME, Sima CS, Riely GJ, Chmielecki J, Kris MG, et al. Acquired resistance to *EGFR* tyrosine kinase inhibitors in *EGFR*-mutant lung cancer: distinct natural history of patients with tumors harboring the T790M mutation. *Clin Cancer Res* 2011;17:1616–22.
- Kosaka T, Yatabe Y, Endoh H, Yoshida K, Hida T, Tsuboi M, et al. Analysis of epidermal growth factor receptor gene mutation in patients with non-small cell lung cancer and acquired resistance to gefitinib. *Clin Cancer Res* 2006;12:5764–9.
- Goebel G, Zitt M, Zitt M, Muller HM. Circulating nucleic acids in plasma or serum (CNAPS) as prognostic and predictive markers in patients with solid neoplasias. *Dis Markers* 2005;21:105–20.
- Vlassov VV, Laktionov PP, Rykova EY. Circulating nucleic acids as a potential source for cancer biomarkers. *Curr Mol Med* 2010;10:142–65.
- Diehl F, Schmidt K, Choti MA, Romans K, Goodman S, Li M, et al. Circulating mutant DNA to assess tumor dynamics. *Nat Med* 2008;14:985–90.
- Shinozaki M, O'Day SJ, Kitago M, Amersi F, Kuo C, Kim J, et al. Utility of circulating B-RAF DNA mutation in serum for monitoring melanoma patients receiving biochemotherapy. *Clin Cancer Res* 2007;13:2068–74.
- Dressman D, Yan H, Traverso G, Kinzler KW, Vogelstein B. Transforming single DNA molecules into fluorescent magnetic particles for detection and enumeration of genetic variations. *Proc Natl Acad Sci U S A* 2003;100:8817–22.
- Pao W, Ladanyi M. Epidermal growth factor receptor mutation testing in lung cancer: searching for the ideal method. *Clin Cancer Res* 2007;13:4954–5.
- Nagai Y, Miyazawa H, Huqun, Tanaka T, Udagawa K, Kato M, et al. Genetic heterogeneity of the epidermal growth factor receptor in non-small cell lung cancer cell lines revealed by a rapid and sensitive detection system, the peptide nucleic acid-locked nucleic acid PCR clamp. *Cancer Res* 2005;65:7276–82.
- Rago C, Huso DL, Diehl F, Karim B, Liu G, Papadopoulos N, et al. Serial assessment of human tumor burdens in mice by the analysis of circulating DNA. *Cancer Res* 2007;67:9364–70.

16. Diehl F, Schmidt K, Durkee KH, Moore KJ, Goodman SN, Shuber AP, et al. Analysis of mutations in DNA isolated from plasma and stool of colorectal cancer patients. *Gastroenterology* 2008;135:489-98.
17. Li M, Chen WD, Papadopoulos N, Goodman SN, Bjerregaard NC, Laurberg S, et al. Sensitive digital quantification of DNA methylation in clinical samples. *Nat Biotechnol* 2009;27:858-63.
18. Kimura H, Kasahara K, Kawaiishi M, Kunitoh H, Tamura T, Holloway B, et al. Detection of epidermal growth factor receptor mutations in serum as a predictor of the response to gefitinib in patients with non-small-cell lung cancer. *Clin Cancer Res* 2006;12:3915-21.
19. Kuang Y, Rogers A, Yeap BY, Wang L, Makrigiorgos M, Vetrand K, et al. Noninvasive detection of EGFR T790M in gefitinib or erlotinib resistant non-small cell lung cancer. *Clin Cancer Res* 2009;15:2630-6.
20. Brevet M, Johnson ML, Azzoli CG, Ladanyi M. Detection of EGFR mutations in plasma DNA from lung cancer patients by mass spectrometry genotyping is predictive of tumor EGFR status and response to EGFR inhibitors. *Lung Cancer* 2011;73:96-102.
21. Bai H, Mao L, Wang HS, Zhao J, Yang L, An TT, et al. Epidermal growth factor receptor mutations in plasma DNA samples predict tumor response in Chinese patients with stages IIIB to IV non-small-cell lung cancer. *J Clin Oncol* 2009;27:2653-9.
22. Inukai M, Toyooka S, Ito S, Asano H, Ichihara S, Soh J, et al. Presence of epidermal growth factor receptor gene T790M mutation as a minor clone in non-small cell lung cancer. *Cancer Res* 2006;66:7854-8.
23. Soh J, Toyooka S, Ichihara S, Suehisa H, Kobayashi N, Ito S, et al. EGFR mutation status in pleural fluid predicts tumor responsiveness and resistance to gefitinib. *Lung Cancer* 2007;56:445-8.
24. Giaccone G, Wang Y. Strategies for overcoming resistance to EGFR family tyrosine kinase inhibitors. *Cancer Treat Rev* 2011;37:456-64.
25. Ercan D, Zejnullahu K, Yonesaka K, Xiao Y, Capelletti M, Rogers A, et al. Amplification of EGFR T790M causes resistance to an irreversible EGFR inhibitor. *Oncogene* 2010;29:2346-56.
26. Schwarzenbach H, Hoon DS, Pantel K. Cell-free nucleic acids as biomarkers in cancer patients. *Nat Rev Cancer* 2011;11:426-37.
27. Diehl F, Li M, Dressman D, He Y, Shen D, Szabo S, et al. Detection and quantification of mutations in the plasma of patients with colorectal tumors. *Proc Natl Acad Sci U S A* 2005;102:16368-73.
28. Margulies M, Egholm M, Altman WE, Attiya S, Bader JS, Bemben LA, et al. Genome sequencing in microfabricated high-density picolitre reactors. *Nature* 2005;437:376-80.
29. Rothberg JM, Hinz W, Rearick TM, Schultz J, Mileski W, Davey M, et al. An integrated semiconductor device enabling non-optical genome sequencing. *Nature* 2011;475:348-52.
30. Kinde I, Wu J, Papadopoulos N, Kinzler KW, Vogelstein B. Detection and quantification of rare mutations with massively parallel sequencing. *Proc Natl Acad Sci U S A* 2011;108:9530-5.



Continuous EGFR-TKI administration following radiotherapy for non-small cell lung cancer patients with isolated CNS failure

Takehito Shukuya^{a,b,*}, Toshiaki Takahashi^a, Tateaki Naito^a, Rieko Kaira^a, Akira Ono^a, Yukiko Nakamura^a, Asuka Tsuya^a, Hirosugu Kenmotsu^a, Haruyasu Murakami^a, Hideyuki Harada^c, Koichi Mitsuya^d, Masahiro Endo^e, Yoko Nakasu^d, Kazuhisa Takahashi^b, Nobuyuki Yamamoto^a

^a Division of Thoracic Oncology, Shizuoka Cancer Center, 1007 Shimonagakubo, Nagaizumi-chou, Suntou-gun, Shizuoka 411-8777, Japan

^b Department of Respiratory Medicine, Juntendo University, School of Medicine, 2-1-1 Hongou, Bunkyo-ku, Tokyo, 113-8421, Japan

^c Division of Radiation Oncology, Shizuoka Cancer Center, 1007 Shimonagakubo, Nagaizumi-chou, Suntou-gun, Shizuoka 411-8777, Japan

^d Division of Neurosurgery, Shizuoka Cancer Center, 1007 Shimonagakubo, Nagaizumi-chou, Suntou-gun, Shizuoka 411-8777, Japan

^e Division of Diagnostic Radiology, Shizuoka Cancer Center, 1007 Shimonagakubo, Nagaizumi-chou, Suntou-gun, Shizuoka 411-8777, Japan

ARTICLE INFO

Article history:

Received 26 January 2011

Received in revised form 29 March 2011

Accepted 5 April 2011

Keywords:

Non-small cell lung cancer

Gefitinib

Resistance

Brain metastasis

Whole brain irradiation

Stereotactic radiosurgery

Beyond PD

ABSTRACT

Introduction: Based on previous reports, patients who experience isolated central nervous system (CNS) failure may not have systemic acquired resistance to EGFR-TKI therapy. However, because there are few articles that have reported on the clinical efficacy of continuous EGFR-TKI administration following progressive disease (PD) in isolated CNS metastasis, we retrospectively investigated the possibility of using the treatment.

Patients and methods: From July 2002 to December 2009, 17 non-small cell lung cancer patients showed isolated CNS failure after clinical benefit (partial response or stable disease longer than 6 months) from EGFR-TKIs and continuously received EGFR-TKIs following radiotherapy (whole brain radiotherapy or stereotactic radiotherapy) to the CNS metastases.

Results: The response rate and the disease control rate of CNS lesions were 41% and 76%, respectively. The median progression free survival, extracranial progression free survival and the median overall survival time were 80 days, 171 days and 403 days, respectively. The toxicities which were observed during the first EGFR-TKI treatments were sustained, but did not worsen during this study period. The acute toxicities caused by radiotherapy to the CNS were controllable. There were no remarkable late toxicities related to the treatment.

Conclusions: Continuous administration of EGFR-TKI following radiotherapy after PD in isolated CNS metastasis appears to be a valid treatment option.

© 2011 Elsevier Ireland Ltd. All rights reserved.

1. Introduction

Gefitinib, one of the epidermal growth factor receptor tyrosine kinase inhibitors (EGFR-TKIs), is one of the options for the first-line treatment of non-small cell lung cancer (NSCLC) patients harboring sensitive EGFR mutations based on the findings of previous clinical trials [1–3]. Despite an initial dramatic response to treatment, the disease eventually progresses in the majority of the patients after a median of about 10 months [1–4].

The central nervous system (CNS) is a common site for metastasis of NSCLC. Patients with CNS metastasis generally suffer from

deterioration of performance status (PS) and, therefore, do not have a long survival time. Lee et al. reported that the CNS is frequently the initial failure site in Korean NSCLC patients showing an initial clinical benefit from EGFR-TKIs, and 13% of their NSCLC patients showed isolated CNS failure after clinical benefit with EGFR-TKIs [5]. In such patients, controlling both brain and systemic lesions is important to maintain or improve their quality of life and to prolong their survival.

Jackman et al. proposed the clinical definition of acquired resistance to EGFR-TKI in order to lead to a more uniform approach to investigating the problem of acquired resistance to EGFR-TKIs [6]. The proposed criteria include the following: 1. a tumor that harbors an EGFR mutation known to be associated with drug sensitivity or objective clinical benefit from treatment with an EGFR TKI; 2. systemic progression of disease (Response Evaluation Criteria in Solid Tumors [RECIST] or WHO) while on continuous treatment with gefitinib or erlotinib within the last 30 days; 3. no intervening

* Corresponding author at: Division of Thoracic Oncology, Shizuoka Cancer Center, 1007 Shimonagakubo, Nagaizumi-chou, Suntou-gun, Shizuoka 411-8777, Japan. Tel.: +81 55 989 5222; fax: +81 55 989 5783.

E-mail address: tshukuya@juntendo.ac.jp (T. Shukuya).

systemic therapy between cessation of gefitinib or erlotinib and initiation of new therapy. However, autopsy reports have shown that CNS metastases may remain free of mutations associated with secondary resistance, despite the development of such mutations in systemic sites of disease [7,8]. Based on these reports, Jackman et al. described that patients who experience isolated CNS failure would not be considered as having systemic acquired resistance to EGFR TKI therapy [6].

However, because only a few articles have reported on the clinical efficacy of continuous EGFR-TKI administration beyond the determination of progressive disease (PD) by isolated CNS metastasis, the efficacy is unclear. At our institute, as Jackman et al. described, we usually administer EGFR-TKI continuously after radiotherapy for the patients with PD in isolated CNS metastasis. In this article, we retrospectively investigated the efficacy of this treatment.

2. Patients and methods

2.1. Patient selection

The study subjects were consecutively registered according to the following inclusion criteria: 1. histological or cytological confirmation of advanced NSCLC; 2. a tumor that harbors an EGFR mutation known to be associated with drug sensitivity or objective clinical benefit (PR or SD longer than 6 months) from treatment with an EGFR TKI; 3. determination of PD in isolated CNS metastasis while on continuous treatment with an EGFR-TKI (gefitinib or erlotinib) within the last 30 days; 4. no intervening systemic therapy between cessation of gefitinib or erlotinib and initiation of radiotherapy for the CNS metastasis; and 5. a willingness to provide written informed consent.

2.2. Treatment methods

After determination of PD in isolated CNS metastasis, stereotactic radiotherapy (SRT) or whole brain radiotherapy (WBRT) were conducted according to the consultation with neurosurgeons and radiation oncologists. EGFR-TKIs (gefitinib or erlotinib) were discontinued during SRT or WBRT. EGFR-TKIs were restarted on the next day after the final day of radiotherapy for the CNS metastases. The selection of the EGFR-TKI (gefitinib or erlotinib) after radiotherapy of the CNS metastases was determined by the physicians in charge. EGFR-TKIs were continued until disease progression, the appearance of intolerable toxicity or withdrawal of consent. Corticosteroids, glycerol or mannitol were also used, depending on the symptoms of brain edema caused by the brain metastasis itself or resulting from radiotherapy applied to the CNS.

3. Evaluation of the response and toxicity

The patients were evaluated to determine the stage of their disease before the start of the treatment as well as at the time of the progression or relapse of the disease. The stage of their disease was determined by a complete medical history and a physical examination, including chest X-ray, CT of the chest and the abdomen, MRI of the head and additional staging procedures such as bone scintigraphy and PET. The tumor response was evaluated in accordance with the response evaluation criteria in solid tumors (RECIST) ver. 1.0. The tumor response in the CNS was evaluated basically by enhanced brain MRI and neurological findings. If there were measurable lesions, the tumor response was evaluated based on the RECIST ver. 1.0. If there were no measurable lesions, the tumor response was evaluated

and classified as PR, SD or PD based on the enhanced brain MRI findings and neurological findings. Carcinomatous meningitis was diagnosed by lumbar puncture, brain MRI or both. To distinguish pseudo-tumor effects occurred with IICP (increased intracranial pressure) signs and controversial brain image findings after cranial radiotherapy from disease progression, the tumor response in the CNS was carefully evaluated by medical oncologists, neurosurgeons and radiologists, taking into account not only enhanced brain MRI and neurological findings but also clinical courses. Acute adverse events were evaluated until 4 weeks after the last administration of EGFR-TKIs or until the patient's death, and late adverse events, especially neurological adverse events like memory impairment and leukoencephalopathy, were evaluated in accordance with the common terminology criteria for adverse events (CTCAE) ver. 3.0.

3.1. Statistical methods

To analyze the progression free survival (PFS), extracranial PFS and overall survival (OS), survival curves were drawn by the Kaplan–Meier method. The PFS was calculated from the date of initiation of the radiotherapy to the date of detection of disease progression or the date of occurrence of death from any cause. PFS was censored at the date of the last visit for those patients who were alive without documented disease progression. The extracranial PFS was calculated from the date of initiation of the radiotherapy to the date of detection of disease progression except CNS metastases during EGFR-TKI treatment, or the date of the occurrence of death from any cause. The extracranial PFS was censored at the date of the detection of isolated CNS disease progression and cessation of EGFR-TKIs, or the date of the last visit for those patients who were alive without documented disease progression.

The OS was calculated from the date of initiation of the radiotherapy to the date of death. OS was censored at the date of the last visit for those patients whose deaths could not be confirmed. PFS were compared using the log-rank test according to the patients' characteristics and treatment modalities (PS: 0–1 vs 2–3, with carcinomatous meningitis vs without carcinomatous meningitis, symptomatic CNS metastases vs asymptomatic CNS metastases, SRT vs WBRT). All of the analyses were performed using the StatView software program, Ver. 5.0 (SAS Institute Inc., Cary, NC, USA).

4. Results

4.1. Patient characteristics and treatment methods

From July 2002 to December 2009, 204 patients met the inclusion criteria (1. histological or cytological confirmation of the advanced NSCLC; 2. a tumor that harbors an EGFR mutation known to be associated with drug sensitivity or objective clinical benefit (PR or SD longer than 6 months) from treatment with an EGFR TKI). Of these 204 patients, 35 patients (17%) showed PD in isolated CNS metastases. Of these 35 patients, 17 patients received radiotherapy for the CNS metastases and continuously received EGFR-TKIs. Most of the other 18 patients were judged to have no indications for radiotherapy because of prior history of radiotherapy to CNS metastases, sizes of CNS lesions for SRT, a poor PS and so on. Table 1 shows the patient characteristics.

Among the 17 patients included in this study, 12 (71%) were female, and their median age was 63 years. Sixteen patients (94%) had adenocarcinoma and 12 patients (71%) were never smokers. In 4 patients (23%), the EGFR mutations were investigated, and were detected to be sensitive EGFR mutations (exon 19 deletion in one patient and exon 21 L858R in 3 patients). Fourteen patients

Table 1
Patients' characteristics.

n = 17		No	%
Gender	Male	5	29
	Female	12	71
Age (year)	Median	63	
	Range	43–74	
Histology	Adeno	16	94
	NOS	1	6
PS	0	3	18
	1	6	35
	2	6	35
	3	2	12
Smoking history	Never	12	71
	Former	5	29
EGFR mutation	Mutant	4	23
	Wild	0	0
	Unknown	13	77
Response to the 1st EGFR-TKI	PR	14	82
	SD longer than 6 months	3	18
No. of prior CTx regimens	0	4	23
	1	9	53
	2	3	18
	3	1	6
CNS lesion before EGFR-TKI	Yes	14	82
	No	3	18
Type of metastases in CNS	MBM	10	59
	MBM+CM	7	41
	No. of MBM	6	35
Neurological symptom	1–5	3	18
	6–10	3	18
	11–20	3	18
	More than 21	5	29
Symptomatic	Symptomatic	8	47
	Asymptomatic	9	53

Abbreviations: No., number; adeno, adenocarcinoma; NOS, not otherwise specified; PS, performance status; EGFR, epidermal growth factor receptor; CTx, chemotherapy; CNS, central nerve system; MBM, multiple brain metastasis; CM, carcinomatous meningitis.

and 3 patients showed PR and SD longer than 6 months, respectively, in the treatment of the first EGFR-TKI. Nine patients (53%) had a PS of 0 or 1, and 8 patients (47%) had a PS of 2 or 3. Four patients (23%) received EGFR-TKIs as a first line chemotherapy and 9 patients (53%) received EGFR-TKIs as a second line chemotherapy. Fourteen patients (82%) had CNS metastases before EGFR-TKI treatment, and 13 patients (76%), 2 patients (12%) and 2 patients (12%) had multiple brain metastases, carcinomatous meningitis and multiple brain metastases plus carcinomatous meningitis, respectively, when they were evaluated as having PD in isolated CNS metastases. The numbers of brain metastases were from 1 to 5 in 6 patients, from 6 to 10 in 3 patients, from 11 to 20 in 3 patients and more than 21 in 5 patients.

Table 2 shows the treatment methods employed. All 17 patients received gefitinib as the first EGFR-TKI. WBRT and SRT were conducted in 9 patients and 8 patients, respectively, after the determination of PD in isolated CNS metastases. In the 9 patients who received WBRT, 7 patients continuously received gefitinib and 2 patients continuously received erlotinib. In the 8 patients who received SRT, 7 patients continuously received gefitinib and one patient continuously received erlotinib. Two of 7 patients who had carcinomatous meningitis received not only radiotherapy but also

Table 2
Treatment method.

n = 17		No	%
Treatment method			
gefitinib → WBRT → gefitinib		7	41
gefitinib → SRT → gefitinib		7	41
gefitinib → WBRT → erlotinib		2	12
gefitinib → SRT → erlotinib		1	6

Table 3
Tumor response.

n = 17		No	%
Tumor response			
PR		7	41
SD		6	35
PD		4	24
Response rate (%)		41	
Disease control rate (%)		76	

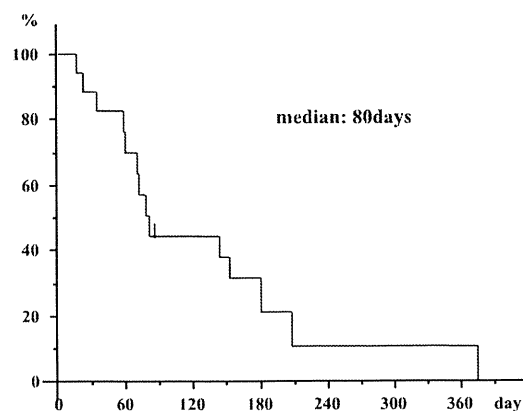


Fig. 1. The Kaplan–Meier curve for progression free survival is shown for the 17 patients. The median progression free survival was 80 days.

intrathecal methotrexate administration and cerebrospinal fluid drainage using Ommaya reservoir.

4.2. Response to therapy, survival and toxicity

Among the 17 patients, 7, 6 and 4 patients showed PR, SD, and PD, respectively. The response rate was 41% and the disease control rate was 76% (Table 3).

The median PFS and the median OS were 80 days and 403 days, respectively (Figs. 1 and 2). There are no statistically significant differences in PFS with regard to the patients' characteristics and treatment modalities (PS: 0–1 vs 2–3, $p=0.186$; with carcinomatous meningitis vs without carcinomatous meningitis, $p=0.336$; symptomatic CNS metastases vs asymptomatic CNS metastases, $p=0.742$; SRT vs WBRT, $p=0.379$). Fig. 3 shows the Kaplan–Meier

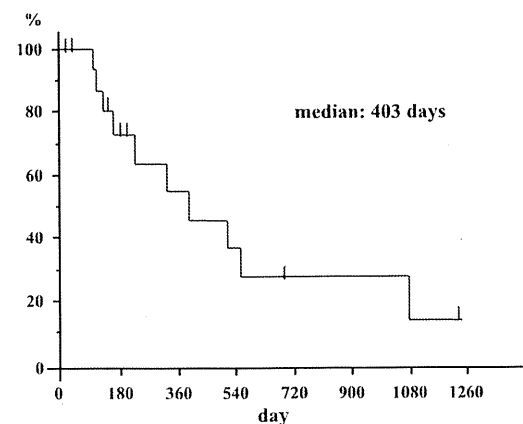


Fig. 2. The Kaplan–Meier curve for overall survival is shown for the 17 patients. The median overall survival was 403 days.

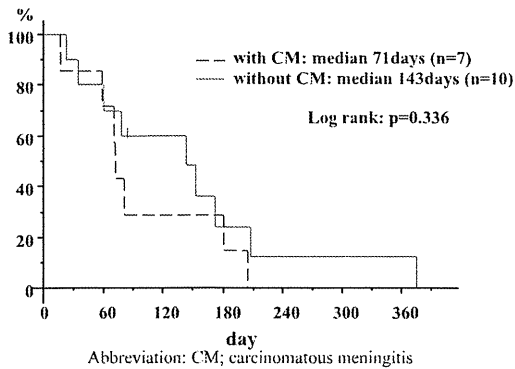


Fig. 3. The Kaplan–Meier curves for progression free survival of the patients with carcinomatous meningitis and without carcinomatous meningitis are shown (with carcinomatous meningitis: dashed line, without carcinomatous meningitis: continuous line). The median PFS were 71 days and 143 days among the patients with carcinomatous meningitis and without carcinomatous meningitis, respectively. Although there were no statistically significant differences, there was a tendency for the patients without carcinomatous meningitis to have a longer PFS than the patients with carcinomatous meningitis. (For interpretation of the references to color in this figure legend, the reader is referred to the web version of this article.)

curves for PFS of the patients with carcinomatous meningitis and without carcinomatous meningitis. The median PFS were 71 days and 143 days among the patients with carcinomatous meningitis and without carcinomatous meningitis, respectively.

The toxicities which were observed during the first EGFR-TKI treatments were continued and not worsened during this study period. Acute toxicities like headache, fatigue and nausea caused by radiotherapy to the CNS were controllable. There were no other remarkable acute or late toxicities related to this study treatment.

4.3. Failure site after continuous EGFR-TKI administration following radiotherapy, extracranial PFS and the treatment after EGFR TKI withdrawal

Table 4 shows the failure sites after radiotherapy of the CNS metastases and continuous treatment with EGFR-TKIs. Among the 17 patients, 5 patients (29%) were evaluated as having PD in the isolated CNS metastases, one patient (6%) had PD in the CNS and other organ metastases. Eight patients (47%) were evaluated to have PD in other organ metastases. Three patients (18%) were still being administered EGFR-TKIs. The median extracranial PFS was 171 days (Fig. 4). Eight patients received other chemotherapeutic regimens after EGFR-TKI withdrawal. The median and average numbers of chemotherapeutic regimens after EGFR-TKI withdrawal were 0 and 1.2, respectively (range: 0–4). Pemetrexed, S-1, docetaxel and amurubicin were administered in 3 patients, 3 patients, 2 patients and 2 patients, respectively, as post EGFR-TKI chemotherapy. Gemcitabine, carboplatin plus paclitaxel and carboplatin plus gemcitabine were administered in one patient, respectively. The median OS of the patients with other chemotherapeutic regimens

Table 4
Failure site after radiotherapy to CNS metastases and continuous treatment of EGFR-TKIs.

n = 17		
Failure site	No	%
CNS only	5	29
CNS + other organ(s)	1	6
Other organ(s)	8	47
Under administration	3	18

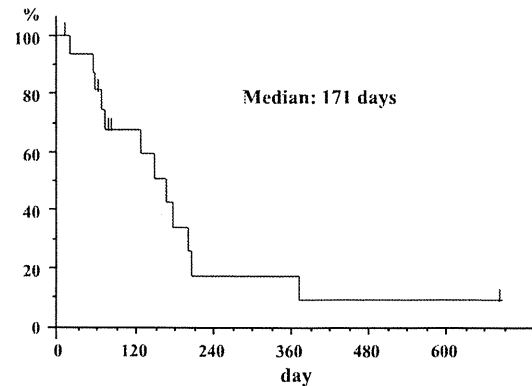


Fig. 4. The Kaplan–Meier curve for extracranial progression free survival is shown for the 17 patients. The median extracranial progression free survival was 171 days.

after EGFR-TKI withdrawal and without those were 564 days and 166 days, respectively (log-rank test, $p = 0.0986$).

5. Discussion

Jackman et al. described that patients who experience isolated CNS failure would not be considered to have systemic acquired resistance to EGFR TKI therapy [6]. However, because there have been only a few articles that have reported on the clinical efficacy of continuous EGFR-TKI administration beyond the determination of PD in isolated CNS metastasis, the efficacy of continuous EGFR-TKI administration beyond the determination of PD is unclear. The present study is useful because it provides a better understanding of the actual efficacy of continuous EGFR-TKI administration beyond the determination of PD in isolated CNS metastases.

The median PFS of the NSCLC patients with PS 0–2 treated by second line pemetrexed or docetaxel was 2.9 months [9]. In the present study, three quarter of the patients received the first EGFR-TKIs as second line or later chemotherapy. The PFS in this study was satisfactory, taking into account the fact that the patients with CNS metastases generally have a poor prognosis [10] and are excluded from clinical trials. Because of the small number of the patients in this study, there are no statistically significant differences in PFS with regard to the patients' characteristics and treatment modalities. However, there were trends toward better PFS for a PS of 0–1 than PS of 2–3 and for the patients without carcinomatous meningitis than with carcinomatous meningitis. The median extracranial PFS in this study was 171 days, and it is therefore considered that continuous EGFR-TKIs can effectively control extracranial disease during this period.

The median survival of untreated lung cancer patients with brain metastasis is approximately 1 month. With treatment, the median survival after diagnosis is approximately 4 months [11]. Although this was reported before the appearance of molecular targeted agents, the OS in this study was satisfactory. There seemed to be a difference between extracranial PFS and OS. Eight patients received other chemotherapeutic regimens after EGFR-TKI withdrawal, and the average number of chemotherapeutic regimens after EGFR-TKI withdrawal was 1.2 (range: 0–4). These post-EGFR-TKI treatments affected the difference between extracranial PFS and OS.

The late adverse events caused by radiotherapy of brain metastases, especially neurological adverse events like memory impairment and leukoencephalopathy, become of increasing concern when the survival time of the patients becomes longer. However, there were no remarkable late toxicities related to this treatment in the present study.

Katayama et al. reported the efficacy of erlotinib for brain and leptomeningeal metastases in patients with lung adenocarcinoma who showed an initial good response to gefitinib [12]. Three of seven patients showed a PR, three had SD, and one had PD. The OS after erlotinib treatment ranged from 15 to 530 days in their study (median, 88 days). They concluded that erlotinib was a reasonable option for the treatment of CNS lesions that appeared after a good initial response of extra-CNS disease to gefitinib. In this study, the response rate, disease control rate and PFS of the patients who received erlotinib as a continuous EGFR-TKI was 67%, 100% and longer than 164 days, respectively. Therefore, switching gefitinib to erlotinib after radiotherapy for CNS metastases might be recommended, especially if the patients received gefitinib as a first EGFR-TKI and are feasible to receive erlotinib.

Lee et al. reported that 13% of NSCLC patients showed isolated CNS failure after initial clinical benefit with EGFR-TKIs [5]. Lee et al. defined “clinical benefit with EGFR-TKIs” as PR or SD with EGFR-TKIs treatment. In the present study, we defined “clinical benefit with EGFR-TKIs” as PR or SD longer than 6 months with EGFR-TKIs based on the definition by Jackman et al. Of the 35 patients who showed PD in isolated CNS metastases, about one-third of the patients received best supportive care alone because of a poor PS. Moreover, the PFS was longer in the patients with a PS of 0–1 than 2–3. Therefore, we should pay special attention to CNS failure and treat patients in an earlier stage in order to maintain or improve their quality of life and to prolong their survival. In addition, prophylactic cranial irradiation in patients with advanced NSCLC who showed clinical benefit with EGFR-TKIs could be a good treatment strategy.

The limitations of this study must be addressed. Although the toxicities observed in this study were expected and controllable, the severity of non-hematologic toxicities, in particular, may have been underestimated in the present study because of its retrospective nature. All of the patients were evaluated for their evaluable lesions approximately every 2 months by CT, MRI, bone scintigraphy or PET. However, the intervals between evaluations in the present study were not as accurate as those in a prospective study.

In conclusion, continuous administration of EGFR-TKI after the determination of PD in isolated CNS metastasis and radiother-

apy for the CNS metastasis might represent an effective treatment option. Further investigations in a larger number of patients are needed to determine whether the treatment used in the present study is actually beneficial or not, and to control CNS failure after the clinical benefit with EGFR-TKIs.

Conflict of interest

None of the authors have any financial or personal relationships that could influence their work.

References

- [1] Mok TS, Wu YL, Thongprasert S, et al. Gefitinib or carboplatin-paclitaxel in pulmonary adenocarcinoma. *N Engl J Med* 2009;361:947–57.
- [2] Mitsudomi T, Morita S, Yatabe Y, et al. Gefitinib versus cisplatin plus docetaxel in patients with non-small-cell lung cancer harbouring mutations of the epidermal growth factor receptor (WJTOG3405): an open label, randomised phase 3 trial. *Lancet Oncol* 2010;11:121–8.
- [3] Maemondo M, Inoue A, Kobayashi K, et al. Gefitinib or chemotherapy for non-small-cell lung cancer with mutated EGFR. *N Engl J Med* 2010;362:2380–8.
- [4] Kosaka T, Yatabe Y, Endoh H, et al. Analysis of epidermal growth factor receptor gene mutation in patients with non-small cell lung cancer and acquired resistance to gefitinib. *Clin Cancer Res* 2006;12:5764–9.
- [5] Lee YJ, Choi HJ, Kim SK, et al. Frequent central nervous system failure after clinical benefit with epidermal growth factor receptor tyrosine kinase inhibitors in Korean patients with non-small-cell lung cancer. *Cancer* 2010;116:1336–43.
- [6] Jackman D, Pao W, Riely GJ, et al. Clinical definition of acquired resistance to epidermal growth factor receptor tyrosine kinase inhibitors in non-small-cell lung cancer. *J Clin Oncol* 2010;28:357–60.
- [7] Balak MN, Gong Y, Riely GJ, et al. Novel D761Y and common secondary T790M mutations in epidermal growth factor receptor-mutant lung adenocarcinomas with acquired resistance to kinase inhibitors. *Clin Cancer Res* 2006;12:6494–501.
- [8] Jackman DM, Holmes AJ, Lindeman N, et al. Response and resistance in a non-small-cell lung cancer patient with an epidermal growth factor receptor mutation and leptomeningeal metastases treated with high-dose gefitinib. *J Clin Oncol* 2006;24:4517–20.
- [9] Hanna N, Shepherd FA, Fossella FV, et al. Randomized phase III trial of pemetrexed versus docetaxel in patients with non-small-cell lung cancer previously treated with chemotherapy. *J Clin Oncol* 2004;22:1589–97.
- [10] Ricciardi S, Marinis FD. Multimodality management of non-small cell lung cancer patients with brain metastases. *Curr Opin Oncol* 2010;22:86–93.
- [11] Nussbaum ES, Djalilian HR, Cho KH. Brain metastases histology, multiplicity, surgery, survival. *Cancer* 1996;78:1781–8.
- [12] Katayama T, Shimizu J, Suda K, et al. Efficacy of erlotinib for brain and leptomeningeal metastases in patients with lung adenocarcinoma who showed initial good response to gefitinib. *J Thorac Oncol* 2009;4:1415–9.

Original Article

Prognosis and Therapeutic Response According to the World Health Organization Histological Classification in Advanced Thymoma

TETSUZO TAGAWA, TAKURO KOMETANI, KOJI YAMAZAKI, TATSURO OKAMOTO, HIROSHI WATAYA, TAKASHI SETO, SEIICHI FUKUYAMA, ATSUSHI OSOEGAWA, FUMIHIKO HIRAI, KENJI SUGIO, and YUKITO ICHINOSE

Department of Thoracic Oncology, National Kyushu Cancer Center, 3-1-1 Notame, Minami-ku, Fukuoka 811-1395, Japan

Abstract

Purpose. The clinical efficacy of the World Health Organization (WHO) classification of thymoma has been reported to be a prognostic factor for patients with thymomas. This study focuses on the relationship between the therapeutic response and the WHO histological classification in patients with advanced thymoma.

Methods. A retrospective review was performed on 22 patients with Masaoka stage III and IV thymoma treated from 1975 to 2007. There were 1, 1, 7, 3, and 10 patients with WHO histological subtypes A, AB, B1, B2, and B3, respectively.

Results. Surgery was performed on 10 patients. There were 2 complete resections, 2 incomplete resections, and 6 exploratory thoracotomies. Of 18 patients with unresectable tumors, 8, 5, and 5 were treated with radiotherapy, chemotherapy, and chemoradiotherapy as the initial therapy, respectively. The response rate in 9 patients with type A-B2 was significantly better than that in 9 patients with type B3 regardless of treatment modality (100% vs 11.1%, $P = 0.0001$). Only the WHO classification was significantly associated with survival, with type B3 having a worse prognosis than A-B2 ($P = 0.01$).

Conclusions. Type B3 thymoma showed a lower response rate to treatments and thus shorter survival. The WHO classification is a good predictive factor for therapeutic response in advanced thymoma.

Key words Thymoma · Mediastinal tumor · WHO classification

Introduction

A complete surgical resection is considered to be the mainstay of treatment for thymoma.^{1–4} However, it is not always achievable in advanced-stage thymoma. Chemotherapy and radiotherapy have significant activity against this tumor.^{5–7} Multimodality treatment including induction chemotherapy or chemoradiotherapy followed by a resection is associated with a favorable outcome in the treatment of advanced thymomas.^{5,8–15} However, no optimal treatment strategy has yet been determined.

Many studies have reported that the histological classification system of thymomas proposed by the World Health Organization (WHO) is a significant prognostic factor for patients with thymomas.^{16–23} However, no study has focused on the relationship between the WHO classification and clinical response to chemotherapy and/or radiotherapy. This study retrospectively reviewed the treatment outcome of stage III and IV thymomas on the basis of the WHO classification and evaluated its clinical relevance.

Patients and Methods

Patients' Characteristics

This study retrospectively reviewed the clinical records of 22 patients with stage III and IV thymoma who were treated at this institution from 1975 to 2007. The clinical and pathological stage of the disease was based on the staging system described by Masaoka et al.²⁴ The histological analysis of the tumor was based on the WHO classification of cell types. A percutaneous biopsy was performed to determine the pathological classification in cases without a surgical resection. The cases diagnosed before the establishment of the WHO classification were re-evaluated by pathologists. Their clinical characteristics and outcomes are shown in Table 1.

Table 1. Characteristics and outcomes of patients

Patient (age in years, sex)	WHO Type	Stage	Autoimmune disease	Initial therapy	Response to initial therapy	Subsequent treatment	Outcome
1 (63, M)	A	III	—	RT	CR		Died, 8mo
2 (45, M)	B3	III	—	S (ET), RT	SD		Died, 17mo
3 (49, M)	B3	III	MG	RT	SD		Died, 66mo
4 (66, M)	B3	IVb	—	S (ET), CRT (ADR)	SD		Died, 67mo
5 (39, M)	B2	IVa	MG	S (ET), RT	CR	CT (ADR)	Died, 122mo
6 (56, F)	B2	IVa	—	S (ET), RT	PR	CT (ADR)	Died, 153mo
7 (50, M)	B3	IVb	—	CRT (VEMT)	SD		Died, 16mo
8 (34, F)	B3	IVa	—	RT	SD	S (R1)	Died, 12mo
9 (62, M)	B3	III	—	CT (ADOC)	SD	RT	Died, 4mo
10 (61, F)	B1	IVa	—	CT (ADOC)	PR	RT	Died, 73mo
11 (39, F)	B1	IVa	PRCA	S (R1)			Died, 137mo
12 (54, F)	B1	IVa	—	S (ET), CT (ADOC)	PR	RT	Alive, 169mo
13 (74, F)	B3	III	PRCA	CT (EVAC)	SD	RT, S (R1)	Died, 24mo
14 (52, M)	B1	III	—	S (R0)			Alive, 145mo
15 (61, F)	B1	III	—	S (R0)			Alive, 132mo
16 (78, F)	B3	IVa	—	RT	SD		Died, 43mo
17 (65, M)	B2	III	—	S (ET), CRT (EC)	PR	CT (PM)	Alive, 55mo
18 (45, F)	B1	IVa	—	CT (PM)	PR		Alive, 2mo
19 (78, M)	B3	IVa	PRCA	RT	PR		Alive, 45mo
20 (43, F)	B3	IVa	—	S (R1)		CT (CP)	Alive, 31mo
21 (32, M)	B1	IVa	—	CRT (cisplatin)	PR	S (ET)	Alive, 22mo
21 (32, M)	AB	IVa	—	CRT (EC)	PR	S (ET)	Alive, 18mo

WHO, World Health Organization; MG, myasthenia gravis; PRCA, pure red cell aplasia; ADOC, cisplatin, doxorubicin, vincristine, cyclophosphamide; ADR, doxorubicin; CP, carboplatin, paclitaxel; EC, etoposide, carboplatin; EVAC, etoposide, vincristine, doxorubicin, cyclophosphamide; PM, cisplatin, amrubicin; VEMT, vincristine, cyclophosphamide, mitomycin C, toyoimycin; CRT, chemoradiotherapy; CT, chemotherapy; RT, radiation therapy; S, surgery; ET, exploratory thoracotomy; R0, complete resection; R1, microscopically incomplete resection; CR, complete response; SD, stable disease; PR, partial response; mo, month

Table 2. Chemotherapy regimen in initial treatment

Therapy	Regimen	n
Chemotherapy	ADOC	3
	EVAC	1
	PM	1
Chemoradiotherapy	EC	2
	VEMT	1
	ADR alone	1
	CDDP alone	1

ADOC, cisplatin, doxorubicin, vincristine, cyclophosphamide; ADR, doxorubicin; CDDP, cisplatin; EC, etoposide, carboplatin; EVAC, etoposide, vincristine, doxorubicin, cyclophosphamide; PM, cisplatin, amrubicin; VEMT, vincristine, cyclophosphamide, mitomycin C, toyoimycin

There were 12 men and 10 women. The median age was 55 (range 32–78) years. There were 8 patients with stage III, 12 patients with stage IVa, and 2 patients with stage IVb. The histological types of thymoma according to the WHO classification were type A, AB, B1, B2, and B3 tumor in 1, 1, 7, 3, and 10 patients, respectively. There were 2 patients with myasthenia gravis and 3 patients with pure red cell aplasia.

Treatment Regimen

The chemotherapy regimens in first-line treatment are shown in Table 2: 50mg/m² of cisplatin (CDDP) and

40mg/m² of doxorubicin (ADR) on day 1, 0.6mg/m² of vincristine (VCR) on day 3, and 700mg/m² of cyclophosphamide (CPA) on day 4 at 4-week interval was the ADOC protocol, 60mg/m² of CDDP on day 1 and 40mg/m² of amrubicin on days 1, 2, 3 at 3-week interval was the PM protocol, and etoposide (VP-16), VCR, ADR, and CPA was the EVAC protocol. The regimens for chemoradiotherapy included the EC protocol of carboplatin (area under the curve = 6) on day 1 and 100mg/m² of VP-16 on days 1, 2, 3 at 3–4-week interval, VEMT (VCR, CPA, mitomycin C, and toyoimycin), ADR alone, and CDDP alone concurrently with 30–61 Gy of radiation (median, 47.4 Gy). Eight patients underwent radiotherapy and the total radiation dose ranged from 30 to 66 Gy (median, 52.1 Gy), and 5 of 8 patients who received radiotherapy as initial therapy received more than 50 Gy.

Tumor Assessment During and After Treatment

The measurability of target lesions at baseline and the response criteria were based on the Response Evaluation Criteria in Solid Tumors (RECIST). The response criteria were categorized as follows. Complete response: the disappearance of all objective evidence of disease on CT for at least 4 weeks; partial response: at least a 30% decrease in the sum of the pleural thickness at

three separate levels; progressive disease: at least 20% increase in the sum of the pleural thickness at three separate levels or the appearance of one or more new lesions; stable disease: neither sufficient shrinkage to qualify for partial response nor a sufficient increase to qualify for progressive disease. The cases diagnosed before the establishment of the RECIST criteria were re-evaluated by two independent reviewers. The response rate was defined as the sum of complete responses and partial responses. A resection was defined as complete (R0) if all gross disease was removed and if all surgical margins were free of the tumor. Incomplete resection (R1) meant that all cancer tissue except pleural dissemination was removed. An exploratory thoracotomy meant that the tumor was judged to be unresectable during the operation and no resection or only a biopsy was performed.

Statistical Analysis

The survival was calculated from the date of the initial treatment until death due to any cause or the last follow-up (censored). The survival curve was made using the Kaplan–Meier method, and statistical differences between survival curves were examined using the log-rank test. The confidence intervals at 5 and 10 years on the survival curve were calculated based on the cumulative hazard function. The impact of the WHO classification on tumor response to treatment was assessed using the χ^2 test. All data were analyzed using Abacus Concepts Survival Tools for StatView (Abacus Concepts, Berkeley, CA, USA).

Results

Treatment

Figure 1 shows a schematic illustration of the treatment strategy. The treatment strategy for advanced thymoma has varied over time. Surgical resection was performed as the primary treatment throughout the study period, when the tumor was judged to be resectable or marginally resectable. Radiotherapy was primarily selected in the period from the 1970s to mid-1980s (patients 1, 2, 3, 5, 6, and 8) for patients with unresectable tumors or those who underwent an exploratory thoracotomy, and some patients concurrently received chemotherapy (patients 4 and 7). Chemotherapy with the ADOC regimen was used instead of radiotherapy in the mid-1980s (patients 9, 10, and 12). However, radiotherapy was performed for elderly patients (patients 16 and 19). Concurrent chemoradiotherapy using cisplatin or carboplatin has been recently introduced (patients 17, 21, and 22).

Surgery was performed in 10 patients. A complete resection (R0) was performed in 2 patients without

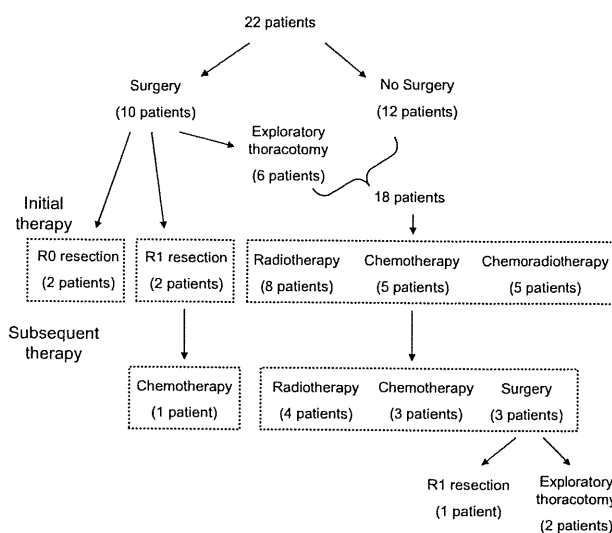


Fig. 1. Schematic illustration of the treatment protocol of the 22 patients with stage III–IV thymomas

adjuvant therapy. An incomplete resection (R1) was performed in 2 patients, due to pleural dissemination followed by chemotherapy in 1 patient. An exploratory thoracotomy was performed in 6 patients. Eighteen patients were treated, including 6 patients who underwent an exploratory thoracotomy; 8 patients were initially treated with radiotherapy, 5 patients with chemotherapy, and 5 patients with chemoradiotherapy. Ten patients were treated with subsequent therapy, including chemotherapy in 3, radiotherapy in 4, and surgery in 3. Subsequent salvage surgery resulted in an R1 resection in 1 patient and an exploratory thoracotomy in 2 patients.

Treatment Response

The responses to the initial therapies are summarized in Table 3. The total response rate was 55.5% in the 18 patients with unresectable tumors. The response rate to the initial therapy of 9 patients with WHO type A–B2 thymomas was significantly higher than that of 9 patients with type B3 tumor (100% vs 11.1%, respectively; $P = 0.0001$). The response rate to each therapy was 60%, 50%, and 60% for chemotherapy, radiotherapy, and chemoradiotherapy, respectively.

Recurrence

Tumor progression after the initial and subsequent therapy was confirmed in 12 patients, with a median progression-free interval of 10 months (range, 5–67 months). The patterns of tumor progression were intrathoracic in 8 patients, distant metastasis in 3 patients, and both

Table 3. Response to initial therapy

WHO type	Therapy						Total	
	Chemotherapy		Radiotherapy		Chemoradiotherapy			
	<i>n</i>	RR, %	<i>n</i>	RR, %	<i>n</i>	RR, %	<i>n</i>	RR, %
A-B2	3	100	3	100	3	100	9	100
B3	2	0	5	20	2	0	18	11.1
Total	5	60	8	50	5	60	18	55.5

RR, response rate

intrathoracic and distant metastasis in 1 patient. One of the two patients who underwent R0 resection had a pleural recurrence 13 months after surgery. The patient underwent extrapleural pneumonectomy (R0 resection) and is now alive with no disease 145 months after the first surgery. The other patient with R0 resection is alive with no recurrence 132 months after surgery.

Survival

At a median follow-up of 61.9 months (range, 1.7–168.7 months), 9 patients were still alive (2 were disease-free) whereas 13 patients died including two nontumor-related deaths. One patient who had type B3 tumor with pure red cell aplasia died of pneumonia 25 months after the initial therapy. The other patient, who also had a type B3 tumor but without autoimmune disease, died of cardiac failure 5 months after the initial therapy. The median survival time was 73 months. The overall survival rates at 5 and 10 years for all patients were 64.9% (95% confidence interval [CI] 39.7%–81.6%) and 43.2% (95% CI 19.2%–65.3%), respectively (Fig. 2). The survival curves of 18 patients who had stage III or IVa disease without R0 resection in relation to the WHO classification are shown in Fig. 3. The 5-year survival rates were 88.9% (95% CI 43.3%–98.4%) for 10 patients with WHO type A-B2 thymomas (excluding 2 patients with R0 resection) and 33.3% (95% CI 9.0%–61.1%) for 8 patients with WHO type B3 tumors (excluding 2 patients with stage IVb disease), which were significantly different ($P = 0.01$). The Masaoka staging system showed the 5- and 10-year survival rates to be 50.0% (95% CI 15.2%–77.5%) and 33.3% (95% CI 5.6%–65.8%) for 8 patients with stage III tumors, and 74.0% (95% CI 38.2%–91.0%) and 37.0% (95% CI 9.1%–66.2%) for 14 patients with stage IV tumors, which were not significantly different. The association of autoimmune diseases was not correlated with the survival.

Discussion

Thymomas are often chemotherapy-sensitive tumors, and therefore chemotherapy has been adopted in patients

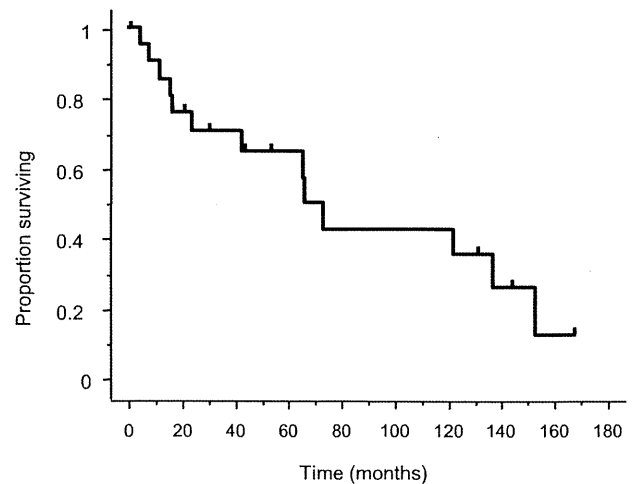


Fig. 2. Overall survival of 22 patients with stage III–IV thymomas. The median survival time was 73 months. The overall survival was 64.9% at 5 years and 43.2% at 10 years

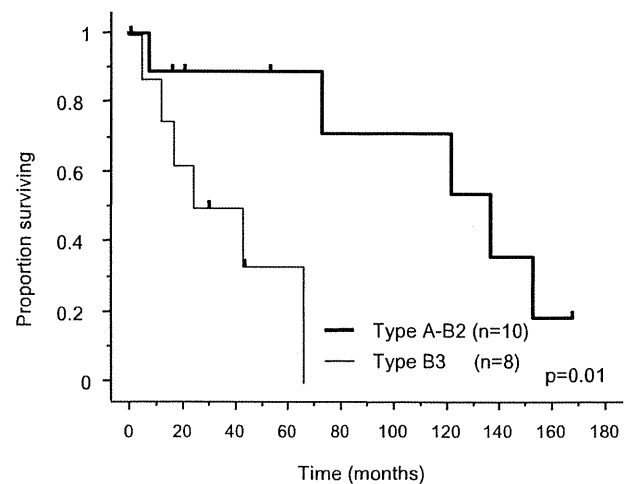


Fig. 3. Survival of 18 patients with stage III or IVa disease without R0 resection according to the World Health Organization histological classification. The 5-year survival rate was 88.9% for 10 patients with type A-B2 and 33.3% for 8 patients with type B3, which showed a significant difference ($P = 0.01$)

with advanced thymomas. Frequently applied agents include cisplatin-based regimens consisting of ADOC, cisplatin, doxorubicin, and cyclophosphamide (PAC), or etoposide, ifosfamide, and cisplatin (VIP). The clinical response rates for unresectable or recurrent thymomas range between 32% and 92%, including 10%–43% of complete response.²⁵ One of the reasons for this wide variation in response rate could be related to the variation in the histology associated with the WHO histological classification. The current study showed that type A-B2 thymoma showed a better response rate to chemotherapy and/or radiotherapy than type B3 thymoma regardless of the treatment modality.

The WHO classification of thymoma is based on morphological features, such as the presence or absence of immature lymphoid components and the degree of cytological atypia. Types AB, B1, and B2 thymomas have a structure similar to that of the cortex in a normal thymus.²⁶ This classification system is a significant prognostic factor for thymoma. Park et al. reported that type B3 and C tumors are associated with poorer survival than the other types of thymoma.¹⁶ Lucchi et al. reported that type B3 thymoma has a more aggressive clinical behavior with a significantly worse prognosis than the other thymomas; however, no correlation is observed between the objective response rate and histological type of disease.²³ Onuki et al. reported that both type B1 and B2 thymomas were significantly better than type B3 thymomas in both radiological and histological radioresponse among 21 patients with stage III thymomas who underwent preoperative radiotherapy.²⁷ They also showed the reduction ratio to be significantly lower in type B3 thymomas than in type B1 or B2 thymomas, and type B3 thymomas did not show obvious histological changes after radiation. Onuki et al. speculated that the difference in the histological changes after radiation between type B2 and B3 thymomas may thus be attributable to the difference in the radioresponse of their epithelial tumor cells.

A genetic analysis of thymic epithelial tumors revealed a relationship between genetic instability and the WHO classification of thymoma. An examination that utilized microsatellite analysis revealed that the incidence of genetic imbalances was more frequent in type B2 and B3 thymomas and thymic carcinoma than in the other types of thymomas.²⁸ Zettl et al. reported that studies using comparative genomic hybridization and fluorescence in situ hybridization showed that genomic aberrations occur frequently in type B3 thymomas.²⁹ Another examination of gene amplification of epithelial growth factor receptor (EGFR) revealed that the average number of EGFR gene signals per cell was higher in type B3 thymomas than in the other types.³⁰ This genetic instability of type B3 thymoma might be related to therapeutic response.

Multimodality treatment including induction chemotherapy for locally advanced thymoma has been recently introduced, and favorable outcomes have been reported.^{5,8–15} The chemotherapeutic regimens administered to date have been diverse and the response rates in these induction settings range from 67% to 100%, while the complete resection rates are reported to be around 70%.^{5,8–10,13} Wright et al. recently reported the results from 10 patients with advanced thymic tumors treated with preoperative concurrent chemoradiation followed by resection.¹⁵ The response rate was 40% and the complete resection rate was 80%. The response rate seemed to be low in comparison to other reports; however, 7 of 10 patients had type B3 thymomas and 1 patient had type C thymoma. Half of the patients who were treated with chemotherapy and/or radiotherapy in the current series had type B3. Although the response rate was 100% in 9 patients with type A-B2 thymoma, the total response rate in 18 patients was 55.5%. It should be noted that response rate could be affected by the ratio of the patients who had type B3 thymoma.

In conclusion, type B3 thymoma showed a lower response rate to treatments and thus a shorter survival. Therefore, the WHO classification is considered to be an effective predictive factor for therapeutic response in advanced thymoma.

Acknowledgment. We thank Ms. Yumiko Oshima for reviewing the patients' charts.

Conflict of Interest Statement. The authors have no conflict of interest or financial support to declare.

References

1. Curran WJ Jr, Kornstein MJ, Brooks JJ, Turrisi AT 3rd. Invasive thymoma: the role of mediastinal irradiation following complete or incomplete surgical resection. *J Clin Oncol* 1988;6:1722–7.
2. Maggi G, Casadio C, Cavallo A, Cianci R, Molinatti M, Ruffini E. Thymoma: results of 241 operated cases. *Ann Thorac Surg* 1991;51:152–6.
3. Thomas CR, Wright CD, Loehrer PJ. Thymoma: state of the art. *J Clin Oncol* 1999;17:2280–9.
4. Kondo K, Monden Y. Therapy for thymic epithelial tumors: a clinical study of 1,320 patients from Japan. *Ann Thorac Surg* 2003;76:878–84.
5. Rea F, Sartori F, Loy M, Calabro F, Fornasiero A, Daniele O, et al. Chemotherapy and operation for invasive thymoma. *J Thorac Cardiovasc Surg* 1993;106:543–9.
6. Loehrer PJ Sr., Perez CA, Roth LM, Greco A, Livingston RB, Einhorn LH. Chemotherapy for advanced thymoma. Preliminary results of an intergroup study. *Ann Intern Med* 1990;113:520–4.
7. Ichinose Y, Ohta M, Yano T, Yokoyama H, Asoh H, Hata K. Treatment of invasive thymoma with pleural dissemination. *J Surg Oncol* 1993;54:180–3.
8. Venuta F, Rendina EA, Longo F, De Giacomo T, Anile M, Mercadante E, et al. Long-term outcome after multimodality treatment for stage III thymic tumors. *Ann Thorac Surg* 2003;76:1866–72.

9. Macchiarini P, Chella A, Ducci F, Rossi B, Testi C, Bevilacqua G, et al. Neoadjuvant chemotherapy, surgery, and postoperative radiation therapy for invasive thymoma. *Cancer* 1991;68:706-13.
10. Kim ES, Putnam JB, Komaki R, Walsh GL, Ro JY, Shin HJ, et al. Phase II study of a multidisciplinary approach with induction chemotherapy, followed by surgical resection, radiation therapy, and consolidation chemotherapy for unresectable malignant thymomas: final report. *Lung Cancer* 2004;44:369-79.
11. Bretti S, Berruti A, Loddo C, Sperone P, Casadio C, Tessa M, et al. Multimodal management of stages III-IVa malignant thymoma. *Lung Cancer* 2004;44:69-77.
12. Lucchi M, Ambrogi MC, Duranti L, Basolo F, Fontanini G, Angeletti CA, et al. Advanced stage thymomas and thymic carcinomas: results of multimodality treatments. *Ann Thorac Surg* 2005;79:1840-4.
13. Jacot W, Quantin X, Valette S, Khial F, Pujol JL. Multimodality treatment program in invasive thymic epithelial tumor. *Am J Clin Oncol* 2005;28:5-7.
14. Evans TL, Lynch TJ. Role of chemotherapy in the management of advanced thymic tumors. *Semin Thorac Cardiovasc Surg* 2005;17:41-50.
15. Wright CD, Choi NC, Wain JC, Mathisen DJ, Lynch TJ, Fidias P. Induction chemoradiotherapy followed by resection for locally advanced Masaoka stage III and IVA thymic tumors. *Ann Thorac Surg* 2008;85:385-9.
16. Park MS, Chung KY, Kim KD, Yang WI, Chung JH, Kim YS, et al. Prognosis of thymic epithelial tumors according to the new World Health Organization histologic classification. *Ann Thorac Surg* 2004;78:992-7.
17. Okumura M, Ohta M, Tateyama H, Nakagawa K, Matsumura A, Maeda H, et al. The World Health Organization histologic classification system reflects the oncologic behavior of thymoma: a clinical study of 273 patients. *Cancer* 2002;94:624-32.
18. Chen G, Marx A, Wen-Hu C, Yong J, Puppe B, Stroebel P, et al. New WHO histologic classification predicts prognosis of thymic epithelial tumors: a clinicopathologic study of 200 thymoma cases from China. *Cancer* 2002;95:420-9.
19. Nakagawa K, Asamura H, Matsuno Y, Suzuki K, Kondo H, Maeshima A, et al. Thymoma: a clinicopathologic study based on the new World Health Organization classification. *J Thorac Cardiovasc Surg* 2003;126:1134-40.
20. Rena O, Papalia E, Maggi G, Oliaro A, Ruffini E, Filosso P, et al. World Health Organization histologic classification: an independent prognostic factor in resected thymomas. *Lung Cancer* 2005;50:59-66.
21. Kondo K, Yoshizawa K, Tsuyuguchi M, Kimura S, Sumitomo M, Morita J, et al. WHO histologic classification is a prognostic indicator in thymoma. *Ann Thorac Surg* 2004;77:1183-8.
22. Kim DJ, Yang WI, Choi SS, Kim KD, Chung KY. Prognostic and clinical relevance of the World Health Organization schema for the classification of thymic epithelial tumors: a clinicopathologic study of 108 patients and literature review. *Chest* 2005;127:755-61.
23. Lucchi M, Melfi F, Dini P, Basolo F, Viti A, Givigliano F, et al. Neoadjuvant chemotherapy for stage III and IVA thymomas: a single-institution experience with a long follow-up. *J Thorac Oncol* 2006;1:308-13.
24. Masaoka A, Monden Y, Nakahara K, Tanioka T. Follow-up study of thymomas with special reference to their clinical stages. *Cancer* 1981;48:2485-92.
25. Girard N, Mornex F, Van Houtte P, Cordier JF, van Schil P. Thymoma: a focus on current therapeutic management. *J Thorac Oncol* 2009;4:119-26.
26. Okumura M, Inoue M, Kadota Y, Hayashi A, Tokunaga T, Kusu T, et al. Biological implications of thymectomy for myasthenia gravis. *Surg Today* 2010;40:102-7.
27. Onuki T, Ishikawa S, Yamamoto T, Ito H, Sakai M, Onizuka M, et al. Pathologic radioresponse of preoperatively irradiated invasive thymomas. *J Thorac Oncol* 2008;3:270-6.
28. Inoue M, Starostik P, Zettl A, Ströbel P, Schwarz S, Scaravilli F, et al. Correlating genetic aberrations with World Health Organization-defined histology and stage across the spectrum of thymomas. *Cancer Res* 2003;63:3708-15.
29. Zettl A, Ströbel P, Wagner K, Katzenberger T, Ott G, Rosenwald A, et al. Recurrent genetic aberrations in thymoma and thymic carcinoma. *Am J Pathol* 2000;157:257-66.
30. Ionescu DN, Sasatomi E, Cieply K, Nola M, Dacic S. Protein expression and gene amplification of epidermal growth factor receptor in thymomas. *Cancer* 2005;103:630-6.

Original Article

Prognosis and Therapeutic Response According to the World Health Organization Histological Classification in Advanced Thymoma

TETSUZO TAGAWA, TAKURO KOMETANI, KOJI YAMAZAKI, TATSURO OKAMOTO, HIROSHI WATAYA, TAKASHI SETO, SEIICHI FUKUYAMA, ATSUSHI OSOEGAWA, FUMIHIKO HIRAI, KENJI SUGIO, and YUKITO ICHINOSE

Department of Thoracic Oncology, National Kyushu Cancer Center, 3-1-1 Notame, Minami-ku, Fukuoka 811-1395, Japan

Abstract

Purpose. The clinical efficacy of the World Health Organization (WHO) classification of thymoma has been reported to be a prognostic factor for patients with thymomas. This study focuses on the relationship between the therapeutic response and the WHO histological classification in patients with advanced thymoma.

Methods. A retrospective review was performed on 22 patients with Masaoka stage III and IV thymoma treated from 1975 to 2007. There were 1, 1, 7, 3, and 10 patients with WHO histological subtypes A, AB, B1, B2, and B3, respectively.

Results. Surgery was performed on 10 patients. There were 2 complete resections, 2 incomplete resections, and 6 exploratory thoracotomies. Of 18 patients with unresectable tumors, 8, 5, and 5 were treated with radiotherapy, chemotherapy, and chemoradiotherapy as the initial therapy, respectively. The response rate in 9 patients with type A-B2 was significantly better than that in 9 patients with type B3 regardless of treatment modality (100% vs 11.1%, $P = 0.0001$). Only the WHO classification was significantly associated with survival, with type B3 having a worse prognosis than A-B2 ($P = 0.01$).

Conclusions. Type B3 thymoma showed a lower response rate to treatments and thus shorter survival. The WHO classification is a good predictive factor for therapeutic response in advanced thymoma.

Key words Thymoma · Mediastinal tumor · WHO classification

Introduction

A complete surgical resection is considered to be the mainstay of treatment for thymoma.¹⁻⁴ However, it is not always achievable in advanced-stage thymoma. Chemotherapy and radiotherapy have significant activity against this tumor.⁵⁻⁷ Multimodality treatment including induction chemotherapy or chemoradiotherapy followed by a resection is associated with a favorable outcome in the treatment of advanced thymomas.^{5,8-15} However, no optimal treatment strategy has yet been determined.

Many studies have reported that the histological classification system of thymomas proposed by the World Health Organization (WHO) is a significant prognostic factor for patients with thymomas.¹⁶⁻²³ However, no study has focused on the relationship between the WHO classification and clinical response to chemotherapy and/or radiotherapy. This study retrospectively reviewed the treatment outcome of stage III and IV thymomas on the basis of the WHO classification and evaluated its clinical relevance.

Patients and Methods

Patients' Characteristics

This study retrospectively reviewed the clinical records of 22 patients with stage III and IV thymoma who were treated at this institution from 1975 to 2007. The clinical and pathological stage of the disease was based on the staging system described by Masaoka et al.²⁴ The histological analysis of the tumor was based on the WHO classification of cell types. A percutaneous biopsy was performed to determine the pathological classification in cases without a surgical resection. The cases diagnosed before the establishment of the WHO classification were re-evaluated by pathologists. Their clinical characteristics and outcomes are shown in Table 1.

Table 1. Characteristics and outcomes of patients

Patient (age in years, sex)	WHO Type	Stage	Autoimmune disease	Initial therapy	Response to initial therapy	Subsequent treatment	Outcome
1 (63, M)	A	III	—	RT	CR		Died, 8mo
2 (45, M)	B3	III	—	S (ET), RT	SD		Died, 17mo
3 (49, M)	B3	III	MG	RT	SD		Died, 66mo
4 (66, M)	B3	IVb	—	S (ET), CRT (ADR)	SD		Died, 67mo
5 (39, M)	B2	IVa	MG	S (ET), RT	CR	CT (ADR)	Died, 122mo
6 (56, F)	B2	IVa	—	S (ET), RT	PR	CT (ADR)	Died, 153mo
7 (50, M)	B3	IVb	—	CRT (VEMT)	SD		Died, 16mo
8 (34, F)	B3	IVa	—	RT	SD	S (R1)	Died, 12mo
9 (62, M)	B3	III	—	CT (ADOC)	SD	RT	Died, 4mo
10 (61, F)	B1	IVa	—	CT (ADOC)	PR	RT	Died, 73mo
11 (39, F)	B1	IVa	PRCA	S (R1)			Died, 137mo
12 (54, F)	B1	IVa	—	S (ET), CT (ADOC)	PR	RT	Alive, 169mo
13 (74, F)	B3	III	PRCA	CT (EVAC)	SD	RT, S (R1)	Died, 24mo
14 (52, M)	B1	III	—	S (R0)			Alive, 145mo
15 (61, F)	B1	III	—	S (R0)			Alive, 132mo
16 (78, F)	B3	IVa	—	RT	SD		Died, 43mo
17 (65, M)	B2	III	—	S (ET), CRT (EC)	PR	CT (PM)	Alive, 55mo
18 (45, F)	B1	IVa	—	CT (PM)	PR		Alive, 2mo
19 (78, M)	B3	IVa	PRCA	RT	PR		Alive, 45mo
20 (43, F)	B3	IVa	—	S (R1)		CT (CP)	Alive, 31mo
21 (32, M)	B1	IVa	—	CRT (cisplatin)	PR	S (ET)	Alive, 22mo
21 (32, M)	AB	IVa	—	CRT (EC)	PR	S (ET)	Alive, 18mo

WHO, World Health Organization; MG, myasthenia gravis; PRCA, pure red cell aplasia; ADOC, cisplatin, doxorubicin, vincristine, cyclophosphamide; ADR, doxorubicin; CP, carboplatin, paclitaxel; EC, etoposide, carboplatin; EVAC, etoposide, vincristine, doxorubicin, cyclophosphamide; PM, cisplatin, amrubicin; VEMT, vincristine, cyclophosphamide, mitomycin C, toyomycin; CRT, chemoradiotherapy; CT, chemotherapy; RT, radiation therapy; S, surgery; ET, exploratory thoracotomy; R0, complete resection; R1, microscopically incomplete resection; CR, complete response; SD, stable disease; PR, partial response; mo, month

Table 2. Chemotherapy regimen in initial treatment

Therapy	Regimen	n
Chemotherapy	ADOC	3
	EVAC	1
	PM	1
Chemoradiotherapy	EC	2
	VEMT	1
	ADR alone	1
	CDDP alone	1

ADOC, cisplatin, doxorubicin, vincristine, cyclophosphamide; ADR, doxorubicin; CDDP, cisplatin; EC, etoposide, carboplatin; EVAC, etoposide, vincristine, doxorubicin, cyclophosphamide; PM, cisplatin, amrubicin; VEMT, vincristine, cyclophosphamide, mitomycin C, toyomycin

There were 12 men and 10 women. The median age was 55 (range 32–78) years. There were 8 patients with stage III, 12 patients with stage IVa, and 2 patients with stage IVb. The histological types of thymoma according to the WHO classification were type A, AB, B1, B2, and B3 tumor in 1, 1, 7, 3, and 10 patients, respectively. There were 2 patients with myasthenia gravis and 3 patients with pure red cell aplasia.

Treatment Regimen

The chemotherapy regimens in first-line treatment are shown in Table 2: 50mg/m² of cisplatin (CDDP) and

40mg/m² of doxorubicin (ADR) on day 1, 0.6mg/m² of vincristine (VCR) on day 3, and 700mg/m² of cyclophosphamide (CPA) on day 4 at 4-week interval was the ADOC protocol, 60mg/m² of CDDP on day 1 and 40mg/m² of amrubicin on days 1, 2, 3 at 3-week interval was the PM protocol, and etoposide (VP-16), VCR, ADR, and CPA was the EVAC protocol. The regimens for chemoradiotherapy included the EC protocol of carboplatin (area under the curve = 6) on day 1 and 100mg/m² of VP-16 on days 1, 2, 3 at 3–4-week interval, VEMT (VCR, CPA, mitomycin C, and toyomycin), ADR alone, and CDDP alone concurrently with 30–61 Gy of radiation (median, 47.4 Gy). Eight patients underwent radiotherapy and the total radiation dose ranged from 30 to 66 Gy (median, 52.1 Gy), and 5 of 8 patients who received radiotherapy as initial therapy received more than 50 Gy.

Tumor Assessment During and After Treatment

The measurability of target lesions at baseline and the response criteria were based on the Response Evaluation Criteria in Solid Tumors (RECIST). The response criteria were categorized as follows. Complete response: the disappearance of all objective evidence of disease on CT for at least 4 weeks; partial response: at least a 30% decrease in the sum of the pleural thickness at